Molecular Crystals and Liquid Crystals Science and Technology. Section A. Molecular Crystals and Liquid Crystals
Publication details, including instructions for authors and subscription information:
http://www.tandfonline.com/loi/gmcl19

Wide-Angle X-ray Scattering Study of Liquid Crystalline Polycarbonates Based on α-Methyl Stilbene Mesogen and Methylene-Containing Flexible Spacer

Y. Y. Cheng [a], M. Brillhart [a b], P. Cebe [a], H. Schreuder-gibson [c], A. Bluhm [c] & W. Yeomans [c]

[a] Department of Materials Science and Engineering, Massachusetts Institute of Technology, Cambridge, MA, 02739

[b] Bonutti Orthopaedic Services, Ltd., Effingham, IL, 62401

[c] U. S. Amy Natick Research, Development and Engineering Center, Natick, MA, 07760

Version of record first published: 24 Sep 2006.

To cite this article: Y. Y. Cheng , M. Brillhart , P. Cebe , H. Schreuder-gibson , A. Bluhm & W. Yeomans (1995): Wide-Angle X-ray Scattering Study of Liquid Crystalline Polycarbonates Based on α-Methyl Stilbene Mesogen and Methylene-Containing Flexible Spacer, Molecular Crystals and Liquid Crystals Science and Technology. Section A. Molecular Crystals and Liquid Crystals, 270:1, 61-75

To link to this article: http://dx.doi.org/10.1080/10587259508031016

Mol. Cryst. Liq. Cryst., 1995, Vol. 270, pp. 61–75
Reprints available directly from the publisher
Photocopying permitted by license only

Wide-Angle X-Ray Scattering Study of Liquid Crystalline Polycarbonates Based on α-Methyl Stilbene Mesogen and Methylene-Containing Flexible Spacer

Y.-Y. CHENG, M. BRILLHART# and P. CEBE*

Department of Materials Science and Engineering, Massachusetts Institute of Technology, Cambridge MA 02139

H. SCHREUDER-GIBSON, A. BLUHM and W. YEOMANS

U. S. Army Natick Research, Development and Engineering Center, Natick, MA 01760

(Received October 6, 1994; in final form Feburary 3, 1995)

Solid state structure has been studied for a series of recently synthesized liquid crystalline polycarbonates[1] based on methyl-substituted stilbene mesogen and methylene-containing flexible spacer. These polymers are referred to as HMS-*n*, where *n* is the number of methylenes in the flexible spacer group. The stability of the liquid crystalline phase and its relationship to the three dimensional crystalline phase were studied. X-ray diffraction patterns of raw fibers drawn from the mesophase revealed that the stability of the mesophase decreases as the methylene spacer length gets close to that of mesogen. From X-ray diffraction patterns of annealed fibers and molecular modeling studies, the unit cell parameters of HMS-5 to 8 were determined. HMS-5 and 6 have an orthorhombic structure while HMS-7 and 8 have a monoclinic structure. More important, an odd-even oscillation is observed in the *d*-spacings of the (0 2 0) and (1 1 0) reflections as a function of *n*, which relates to differences in interchain packing in the odd and even members of the series. All HMS-5 to 8 have a stable intermeshed crystal structure in which the mesogen and the flexible spacer group on adjacent chains are aligned. In this structure, the disposition of the carbonate group differs from *n*-even to *n*-odd, and is responsible for the odd-even effect seen in the two dominant interchain *d*-spacings. We suggest the higher degree of overlap of the carbonate linkage of HMS-7 and 8 might be the reason for their less stable mesophase compared with HMS-5 and 6.

Keywords: Liquid crystalline polymers, thermotropic, X-ray scattering, odd-even effect.

1. INTRODUCTION

Main chain thermotropic liquid crystalline polymers (LCPs) consisting of a rigid mesogen alternating with a flexible spacer have been studied extensively. Stilbene-containing polymers have been widely studied because of the straightforward synthesis of the stilbene, which was evaluated as a synthetic bovine hormone.[2] α-methyl substituted stilbene (HMS) has been used as a mesongenic unit to form LCPs containing methylene units as the flexible spacer. The linking group between the

Present address: Bonutti Orthopaedic Services, Ltd., Effingham, IL 62401
* To whom correspondence should be addressed

mesogen and the flexible spacer may be an ether,[3] an ester,[4,5] or, in our research program, a carbonate.[6] The structural formula for our liquid crystalline polycarbonates is:

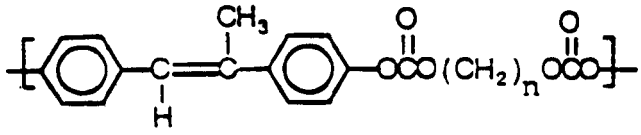

The flexible spacer number, n, ranges from $n = 4$–$10, 12$. We will refer to these polycarbonate based LCPs as HMS-n.

Although both α-methyl stilbene polyethers[3] and α-methyl stilbene polyesters[4,5] are enantiotropic LCPs, our recent study of α-methyl stilbene polycarbonates showed that these LCPs only have a monotropic liquid crystalline phase.[6] Similar monotropic liquid crystalline behavior of other main chain thermotropic LCPs has been observed.[7–15] The distinction is made based on whether or not the mesophase (lc) is stable and can be observed separately from the crystalline phase (k) during cooling from the isotropic (i) melt or during heating.[16] In enantiotropic LCPs, the mesophase is stable with respect to the crystalline phase, and both thermal transitions can be observed in heating and cooling. In other words, $T_{i\text{-}lc}$ and $T_{lc\text{-}k}$ (in cooling) and $T_{k\text{-}lc}$ and $T_{lc\text{-}i}$ (in heating) can be separately identified. In monotropic LCPs, the mesophase is not stable with respect to the crystalline phase. During heating, the $T_{lc\text{-}i}$ transition is always masked by the crystalline melting transition; and, during cooling, the $T_{i\text{-}lc}$ transition can be observed only provided that crystallization is suppressed. In our previous research, we have shown that changing the linking group to carbonate is sufficient to alter the stability of the mesophase, resulting in a monotropic liquid crystalline phase.[6]

In addition to the difference in stability range of the mesophase, there are also differences in the observed odd-even effect between the HMS-polyethers/polyesters and our polycarbonates. The odd-even effect refers to the oscillation of certain parameters as a function of whether the flexible spacer number n is odd or even. An odd-even effect is usually seen for main chain thermotropic LCPs[17–22] in such properties as 1) the transition temperatures $T_{k\text{-}lc}$, $T_{lc\text{-}i}$; 2) the heats of transition, $\Delta H_{lc\text{-}i}$; and 3) the entropy factor, $\Delta S_{lc\text{-}i}$. This phenomenon has been observed for α-methyl stilbene polyethers[3] and α-methyl stilbene polyesters.[4,5] In our HMS polycarbonates, the monotropic nature of the mesophase prevents observation of some of the thermal transitions.[6] Therefore, the odd-even effect in the thermal properties is not obvious because of their monotropic liquid crystalline behavior.[6] However, we did observe that all transition temperatures dropped when n exceeded eight.[6] In addition, in our HMS polycarbonates an interesting odd-even effect has been observed (and reported in preliminary form)[23] in the two dominant interchain d-spacings from the wide angle X-ray scattering powder diffraction pattern when n ranges from 5 to 8. When n exceeded eight, the major interchain d-spacings leveled off.

HMS polyethers, polyesters, and polycarbonates all contain the same stilbene mesogen and the same flexible spacer group. These LCPs differ only in their linking groups. The question arises concerning the aspects of chain structure that cause our HMS polycarbonates to be monotropic LCPs, and to show weak (or no) odd-even

effect in their thermal transitions, compared to their chemical relatives. We suggested previously that the stability of the liquid crystalline phase is affected by the carbonate linkage, which causes fast crystallization resulting from intermolecular interaction.[6] In this work, we explore this idea further by a combined approach using wide angle X-ray scattering and molecular modeling. We show in this work that the HMS polycarbonate chains pack together in an intermeshed structure. The disposition of the carbonate group differs from *n*-even to *n*-odd, and this we suggest is responsible for the odd-even effect in the two dominant interchain *d*-spacings from the wide angle X-ray scattering powder diffraction pattern when *n* ranges from $n = 5$ to 8.

2. EXPERIMENTAL SECTION

The synthesis of HMS polycarbonates followed the method of Sato[24] and has been published separately.[1] The resultant LCPs were soluble in chloroform and obtained as fine white powders, except for $n = 7, 9$ which were obtained as white, very fibrous product. All polymers studies in this research have reasonably high weight average molecular weight, in the range from 11,000 to 54,800 with distributions (M_w/M_n) close to 2.[1]

Wide angle X-ray scattering, WAXS, studies were made in reflection mode for all unoriented HMS polycarbonates. A Rigaku RU-300 rotating anode X-ray generator was used to examine samples in $\theta/2\theta$ reflection mode. The diffractometer has a diffracted beam graphite monochromator. Copper K_α radiation ($\lambda = 1.54$ Å) was used with a step scan interval of 0.1 degree, at a scan rate of 1 degree/minute over the 2θ range from 3 to 53 degrees. HMS powder was melted on a teflon substrate then cooled, and the resulting solid piece was fixed to an aluminum frame for examination by WAXS.

WAXS in transmission mode was performed at room temperature on selected oriented HMS fibers, using a Philips PW 1830 X-ray generator operated by 45 kV and 45 mA with Ni-filtered CuK_α radiation. The Statton camera used in this study consists of a pinhole collimator over which the sample is placed, and a flat film (Kodak DEF-5) to record the scattering pattern. The sample to film distance is calibrated using Si powder reference standard (from National Institute of Standards & Technology) rubbed on the sample surface. The first 2θ value for Si is 28.44°. HMS fibers were hand drawn from the mesophase using tweezers. It was relatively easy to draw fibers for HMS-5, 7, and 8 but quite difficult to draw HMS-6. The hand drawn fibers cooled rapidly in air, and will be referred to as raw fiber. Raw fibers were subsequently annealed below the melting temperature. WAXS was performed on both the raw and annealed fibers.

CERIUS™, a commercial software package distributed by Molecular Simulations Inc., was used for indexing of experimental X-ray diffraction patterns and determination of the crystal structure. Because the experimental *c*-axis repeat unit is close to the end to end distance of the fully extended monomer unit, a initial structure close to all-trans conformation was assumed for X-ray diffraction simulation work. By comparing the experimental powder and oriented fiber diffraction pattern with the simulated patterns, we first determined the crystalline cell symmetry and then refined the crystal lattice parameters.

3. RESULTS AND DISCUSSION

The WAXS diffractometer scans of HMS-5-12 are shown in Figure 1. WAXS scans in reflection mode generally show two sharp and dominant interchain reflections. In addition, several HMS polycarbonates show a number of much weaker peaks. Considering only the two dominant interchain reflections, we show in Figure 2a a plot of

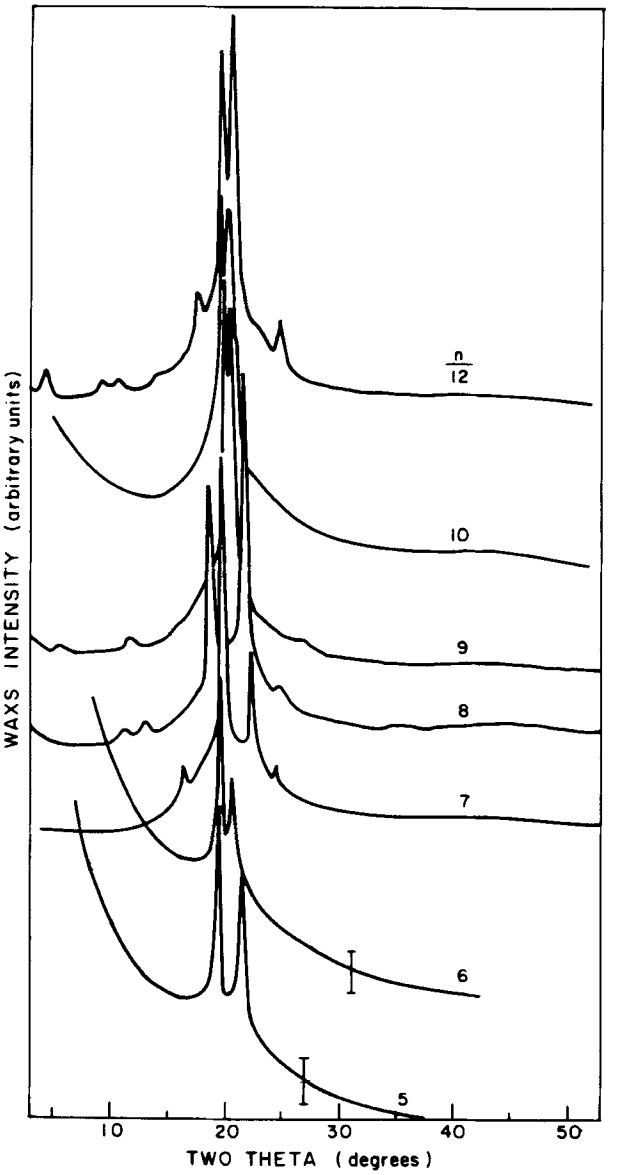

FIGURE 1 WAXS intensity versus two theta for HMS-4-10, -12.

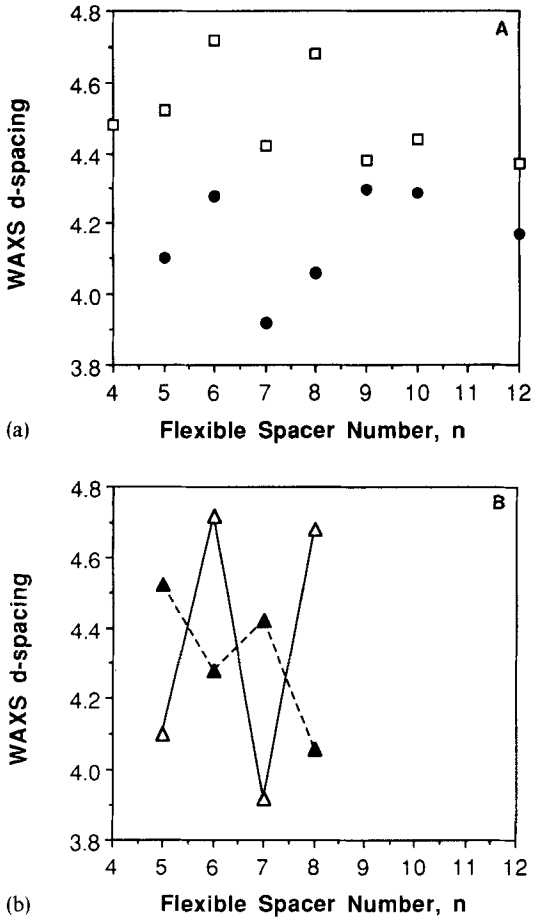

FIGURE 2 Interplanar spacing, d, versus flexible spacer number, n, for HMS polymers. a) (□) higher value d-spacing and (●) lower value d-spacing for the two major interchain reflections shown in Figure 1. b) (——) (020) and (– – – –) (110) interchain reflections grouped according to their Miller indices.

d-spacing vs. flexible spacer number, n. An odd-even effect is observed in both the higher and lower d-spacings for $n = 5$ to 8. When $n \geq 9$, the two major d-spacings get closer to one another and level off. In Figure 2b, the d-spacings are shown for $n = 5$ to 8, designated according to their Miller index assignment. The assignment of Miller indices of (020) and (110) will be explained later.

Next, we show the flat film fiber patterns of raw (unannealed) fibers, and annealed fibers. In Figure 3 WAXS of selected raw fibers are shown. HMS-5 raw fiber is shown in Figure 3a and HMS-8 is shown in Figure 3b. HMS-5 raw fiber WAXS shows a single diffuse equatorial maximum and no meridional reflections, which is characteristic of a nematic mesophase. HMS-8 raw fibers have two diffuse equatorial reflections and no meridional reflections. The appearance of two diffuse equatorial maxima in HMS-8 indicates a better interchain registry between the polymer chains in these fibers. For the

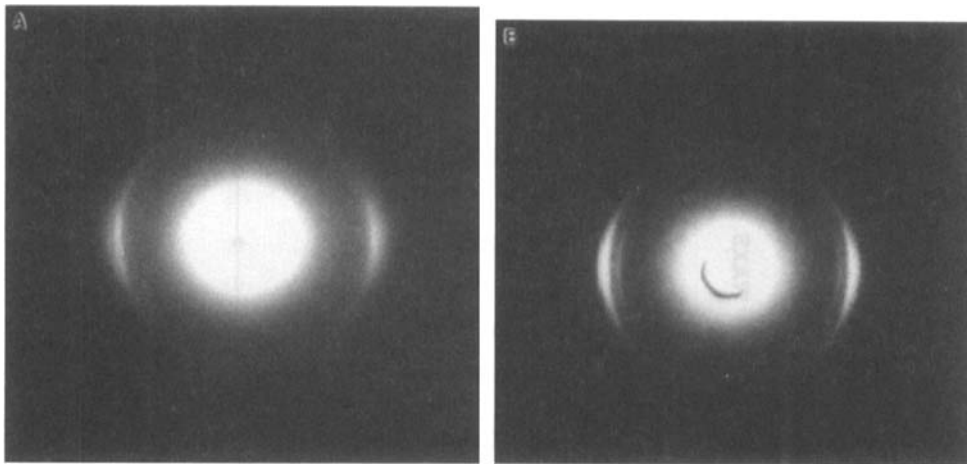

FIGURE 3 Flat film WAXS of hand drawn raw fibers: a) HMS-5, b) HMS-8. Fiber axis is vertical.

sake of brevity, HMS-6 and HMS-7 are not shown. HMS-6 raw fiber was similar to HMS-5, and HMS-7 was similar to HMS-8.

WAXS patterns of selected annealed HMS fibers are shown in Figure 4. Once the raw fiber is annealed, crystalline reflections are observed though some are too weak to be seen in the reproduction. In Figure 4a, HMS-5 annealed fiber WAXS is shown along with a sketch of the reflections in Figure 4b. One meridional reflection is seen in annealed HMS-5 along with two equatorial and five quadrantal reflections. In Figure 4c, annealed fiber WAXS of HMS-8 is shown, with a sketch in Figure 4d. Three

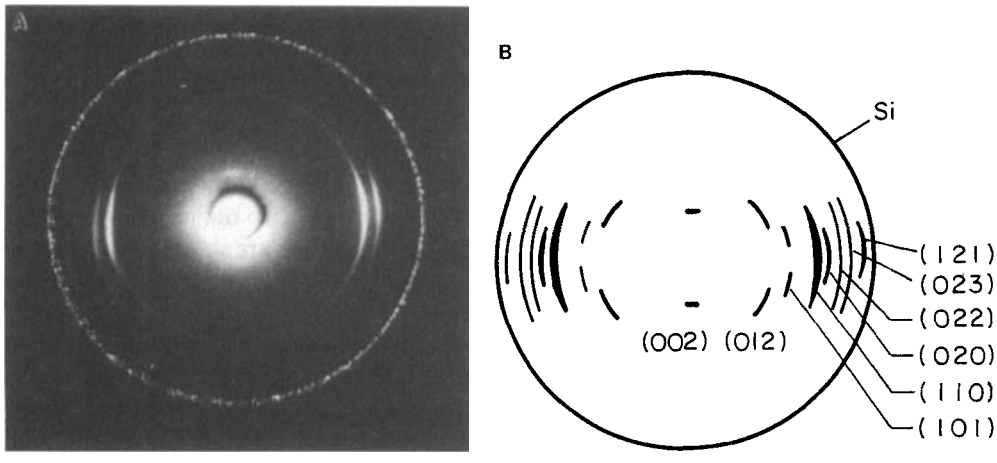

FIGURE 4 WAXS of hand drawn annealed fibers: a) HMS-5 experimental pattern, b) Sketch of HMS-5 pattern, c) HMS-8 experimental pattern, d) Sketch of HMS-8 pattern. Fiber axis is vertical. Spotty ring is from Si calibration standard.

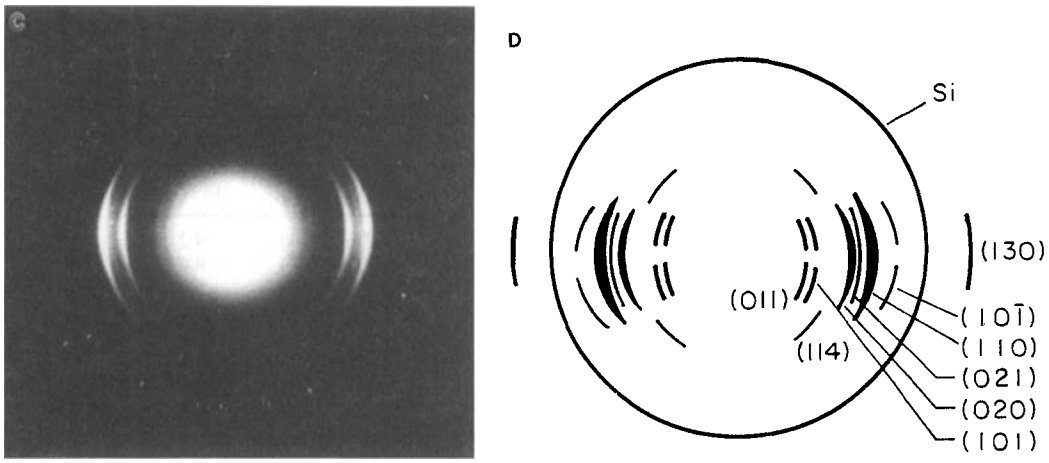

FIGURE 4 *(Continued).*

equatorial and five quadrantal reflections are identified in HMS-8. There were no meridional reflections in HMS-8. HMS-6 and HMS-7 patterns are not shown. HMS-6 did not form highly oriented fibers upon annealing, though numerous crystalline reflections were seen as broad arcs. HMS-7 annealed fiber pattern is similar to that of HMS-8. The experimental 2θ angles and corresponding d-spacings for HMS-5, 6, 7, and 8 are listed in Table 1–4, respectively, for the annealed fibers.

In the raw fibers shown in Figure 3, there is an absence of three dimensional crystalline order. Two raw fibers, HMS-5 and 6, showed a single equatorial reflection, an indication that the nematic mesophase could be described by a single average interchain separation distance. The other two raw fibers, HMS-7 and 8, displayed two strong equatorial reflections, an indication that for these fibers the nematic mesophase

TABLE 1

Experimental and Model Crystallographic Parameters of a Crystal Unit Cell of HMS-5

Miller Index* (h k l)	2θ(°)		d-spacing (Å)	
	data	model	data	model
(1 0 1)	16.4(±0.2°)	16.6	5.4(±0.1 Å)	5.4
(1 1 0)	19.9(±0.2°)	19.8	4.5(±0.1 Å)	4.5
(0 2 0)	22.2(±0.6°)	22.8	4.0(±0.1 Å)	3.9
(0 0 2)	7.6(±0.2°)	7.6	11.6(±0.2 Å)	11.7
(0 1 2)	14.3(±0.6°)	13.7	6.2(±0.3 Å)	6.5
(1 2 1)	27.7(±0.6°)	28.3	3.2(±0.1 Å)	3.2
(0 2 2)	24.6(±0.5°)	24.1	3.6(±0.1 Å)	3.7
(0 2 3)	25.7 (±0.3°)	25.5	3.5(±0.1 Å)	3.5

* Miller indices are assigned based on orthorhombic structure with lattice parameters given in Table 5

TABLE 2

Experimental and Model Crystallographic Parameters of a Crystal Unit Cell of HMS-6

Miller Index* (h k l)	2θ(°)		*d*-spacing (Å)	
	data	model	data	model
(1 1 0)	21.3(±0.3°)	21.2	4.2(±0.1 Å)	4.2
(0 2 0)	19.3(±0.2°)	19.3	4.6(±0.1 Å)	4.6
(0 1 2)	12.2(±0.2°)	12.0	7.2(±0.1 Å)	7.3
(0 1 3)	14.9(±0.4°)	14.5	5.9(±0.2 Å)	6.1
(1 3 1)	35.3(±0.5°)	34.9	2.5(±0.1 Å)	2.6
(0 1 4)	16.7(±0.6°)	17.4	5.3(±0.2 Å)	5.1
(1 1 4)	25.8(±0.3°)	25.8	3.5(±0.1 Å)	3.5
(1 3 4)	38.7(±0.6°)	38.0	2.3(±0.1 Å)	2.4

* Miller indices are assigned based on orthorhombic structure with lattice parameters given in Table 5

TABLE 3

Experimental and Model Crystallographic Parameters of a Crystal Unit Cell of HMS-7

Miller Index* (h k l)	2θ(°)		*d*-spacing (Å)	
	data	model	data	model
(1 0 1)	12.2(±0.2°)	12.1	7.3(±0.1 Å)	7.3
(1 1 0)	20.0(±0.3°)	20.2	4.4(±0.1 Å)	4.4
(1 1 1)	16.5(±0.2°)	16.5	5.4(±0.1 Å)	5.4
(0 2 0)	22.6(±0.3°)	22.5	3.9(±0.1 Å)	4.0
(1 0 2)	9.5(±0.2°)	9.5	9.3(±0.1 Å)	9.3
(1 1 2)	14.7(±0.2°)	14.7	6.0(±0.1 Å)	6.0
(1 2 1)	24.9(±0.6°)	25.6	3.6(±0.1 Å)	3.5
(0 2 2)	26.0(±0.4°)	25.7	3.4(±0.1 Å)	3.5
(2 1 6)	24.0(±0.3°)	23.9	3.7(±0.1 Å)	3.7

* Miller indices are assigned based on monoclinic structure with lattice parameters given in Table 5

would best be described by two different average interchain separation distances. These probably reflect a higher level of order in the packing for HMS-7 and 8. When the three dimensional crystals form out of the nematic phase, which serves as the template on which crystals will nucleate, the average interchain spacing of the crystals is represented by the two strong equatorial reflections which are associated with the (020) and (110) planes.

The interchain spacing of the nematic mesophase seen in the raw fiber WAXS (Figure 3) can be compared to the interchain spacings of the crystalline phase seen in the annealed fiber WAXS (Figure 4). For HMS-5 (Figure 3a) and HMS-6 (not shown) the single equatorial reflection seen in the pattern of the raw, unannealed fiber has

TABLE 4

Experimental and Model Crystallographic Parameters of a Crystal Unit Cell of HMS-8

Miller Index* (h k l)	2θ(°)		d-spacing (Å)	
	data	model	data	model
(0 1 1)	11.4(±0.2°)	11.5	7.8(±0.2 Å)	7.7
(1 0 1)	13.5(±0.5°)	14.0	6.6(±0.3 Å)	6.3
(1 1 0)	21.9(±0.4°)	21.5	4.1(±0.1 Å)	4.1
(0 2 0)	19.0(±0.2°)	19.1	4.7(±0.1 Å)	4.7
(0 2 1)	20.6(±0.4°)	20.2	4.3(±0.1 Å)	4.4
(1 3 0)	34.8(±0.3°)	34.8	2.6(±0.1 Å)	2.6
(1 0 $\bar{1}$)	25.9(±0.3°)	25.2	3.6(±0.1 Å)	3.5
(1 1 4)	16.6(±0.2°)	16.6	5.3(±0.1 Å)	5.3

* Miller indices are assigned based on monoclinic structure with lattice parameters given in Table 5

a d-spacing which lies in between the d-spacings of the two strongest reflections seen in the annealed fiber powder pattern. The inner spot on the equator of HMS-8 raw fiber pattern (Figure 3b), lies on the (0 2 0) position of annealed fiber pattern (Figure 4b). The outer diffuse spot has a d-spacing which lies in between the d-spacings of the two strongest reflections seen in the powder pattern just as the single equatorial reflection does in the HMS-5 and 6 raw fiber pattern. In contrast, the two spots on the each side of equator in the HMS-7 raw fiber pattern have d-spacings close to the d-spacings of the two strongest reflections seen in the powder pattern. For annealed fibers HMS-8 (Figure 4b) and HMS-7 (not shown) the d-spacings of the two strongest equatorial reflections correspond to the two strongest reflections observed in the powder patterns of Figure 1.

Molecular modeling and X-ray simulation work was undertaken to determine the unit cell lattice parameters and crystal structure of the HMS polycarbonates that could be obtained as highly oriented fibers. Crystal structure was determined for HMS-5 through 8. We found the experimental c-axis repeat unit was very close to the end to end distance of a fully extended monomer unit. Therefore, an initial structure with a conformation close to all-trans was used to build the unit cell for X-ray diffraction simulation by CERIUS™. By comparing the experimental powder and oriented fiber diffraction patterns with the simulated patterns, we derive the crystal structures for these polymers. HMS-5 and 6 have an orthorhombic structure with two chains per cell, while HMS-7 and 8 have a monoclinic structure, also with two chains per cell. Figure 5a–c contain the a-b, a-c, and b-c projections, respectively, of HMS-5.

Agreement of intensity between the experimental and simulated X-ray diffraction patterns required the crystal unit cells of HMS-5 through 8 to have two polymer chains at (0,0,0) and (1/2, 1/2, 1/2) positions. Miller indices were assigned using the model lattice parameters. The predicted scattering angle, 2θ, and d-spacings are shown in Tables 1–4 for HMS-5-8, respectively, for direct comparison with the experimental data. Excellent agreement is obtained between the model and experimental d-spacings.

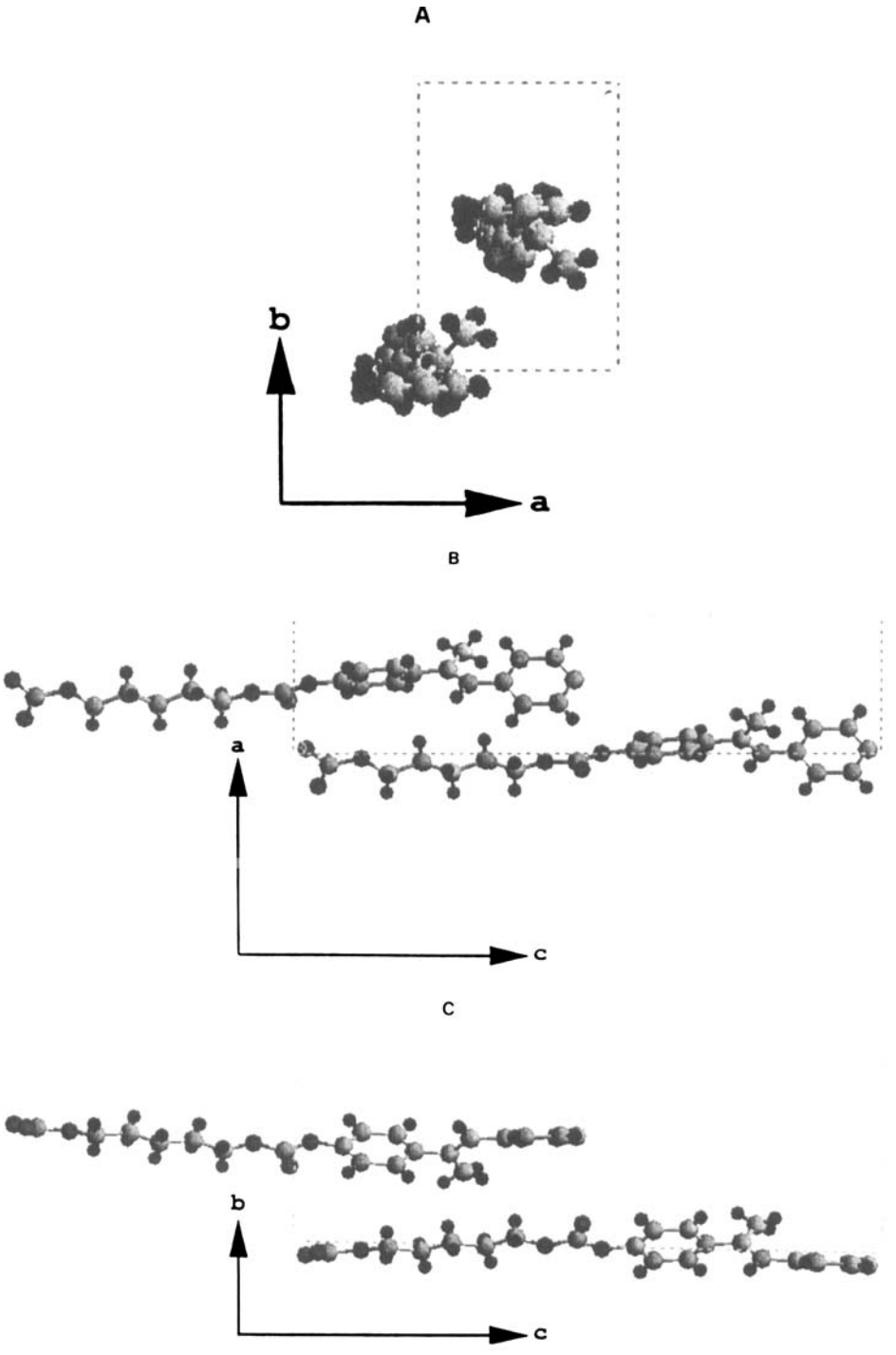

FIGURE 5 Projection of model unit cell of HMS-5 in the a) *a-b* plane b) *a-c* plane and c) *b-c* plane.

In Table 5, we list crystal lattice parameters, a, b, c and angles α, β, γ, for HMS-5 through 8. The last column of the table lists the value of $a \sin \beta$.

The length of the b-axis of the unit cells shows an odd-even alternation for $n = 5$ to 8. In the orthorhombic system (for HMS-5 and 6) the lengths of the a- and b-axes are an indication of the interchain separation distances for the corner chains of the unit cell. For the monoclinic system (HMS-7 and 8), the quantity $a \sin \beta$ represents the perpendicular distance between the corner chains lying in the a–c plane. An odd-even alternation is observed in $a \sin \beta$ for $n = 5$ to 8. This odd-even alternation in parameters b and $a \sin \beta$ causes the d-spacings of the (020) and (110) reflections to alternate, as shown before in Figure 2b.

In the crystal unit cell, HMS-5-8 have an extended chain structure. In Figure 6a–b we show the extended chain structures for monomer units of HMS-5 and 6, respectively. Note that for odd numbered n the two carbonyl oxygens lie on the same side of the monomer chain axis, while for even numbered n they lie on opposite sides of the chain as shown by the arrows. The carbonate linkage, which distinguishes this HMS series from the HMS-polyethers and HMS-polyesters, has important consequences for the unit cell symmetry, chain packing, and mesophase stability. When HMS-polycarbonate monomers pack into the crystalline unit cell, the crystal symmetry is such that the center chain occupies a position shifted along the molecular chain axis, relative to the position of the corner chain. This causes HMS-5 to 8 have an *intermeshed* structure, which is similar to that observed in other main chain LCPs.[25,26] In Figure 7 the corner and center chains of the unit cell of HMS-7 are shown in a projection along the b-c plane. As seen in Figure 7, in the intermeshed crystal, showing a center and corner chain, the stilbene mesogen of one chain is adjacent to the flexible spacer group of the neighboring chain.

A stable intermeshed structure can exist if the length of the flexible spacer is not too large compared with the length of the mesogen, as suggested by Unger and Keller.[25] The methyl stilbene mesogen has a unit length of about 11.6 Å. We can categorize the HMS-polycarbonates into three groups according to the relative lengths of the mesogen and the other portions of the chain. First, HMS-4 has a length of flexible spacer and linking groups of 10.8 Å that is quite short compared to the methyl stilbene mesogen. DSC studies show that while HMS-4 forms a nematic mesophase, the short flexible spacer group causes very slow crystallization kinetics.[6] Very poor crystals form over a wide temperature range from the melt, leading to very low ultimate degree of

TABLE 5

Crystal Lattice Parameters of HMS-5-8*

Sample n	a(Å)	b(Å)	c(Å)	α(°)	β(°)	γ(°)	$a \sin \beta$
5	5.5	7.8	23.4	90.0	90.0	90.0	5.5
6	4.7	9.2	24.4	90.0	90.0	90.0	4.7
7	9.4	7.9	25.6	90.0	34.3	90.0	5.3
8	9.1	9.3	26.8	90.0	30.4	90.0	4.6

* determined from model structure

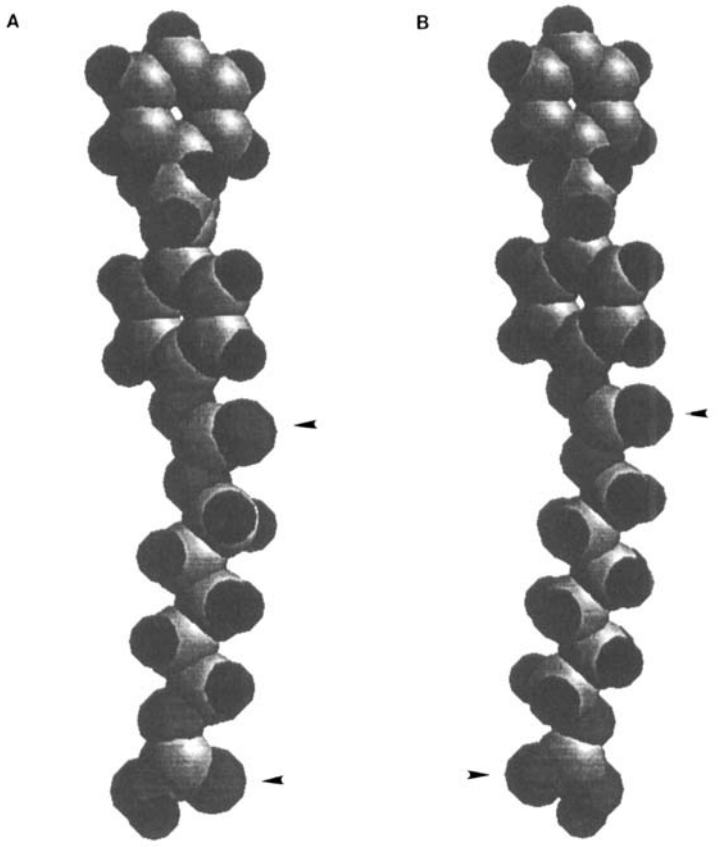

FIGURE 6 Model repeat unit structures for HMS-*n*: a) HMS-5, b) HMS-6.

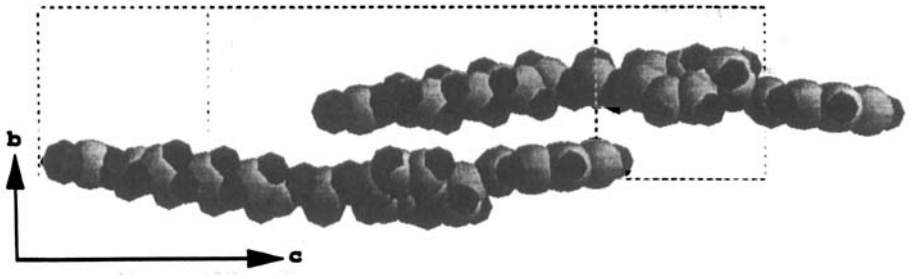

FIGURE 7 Disposition of the corner and center chains of the unit cell, viewed in projection in the *b*-*c* plane for HMS-7.

crystallinity. In the second group, HMS-9, 10 and 12 have flexible spacer lengths ranging from 12.6 Å to 16.5 Å, which are all very long compared to the methyl stilbene mesogen. As shown in Figure 2, the interchain *d*-spacings level off when $n \geq 9$. Furthermore, for $n \geq 9$ no large spherulites were seen with polarized optical micro-

scopy and transition temperatures observed in DSC cooling and heating scans drop sharply.[6] These facts suggest that crystal size and perfection are reduced for HMS-9, 10 and 12. Here the flexibility of the chain leads to rapid crystallization kinetics and relatively less perfect crystals. However, the intermeshed structure is not stable in these members of the series. The flexible spacer is too long to allow proper overlap of the carbonates on adjacent chains.

Finally, in the third group are the series members HMS-5 through 8 in which the length of the mesogen is close to the length of the other groups, leading to a favorable overlap of the adjacent carbonates. HMS-8 has a stable intermeshed crystal structure, because the extended -$(CH_2)_8$- length is about 11.3 Å which is close to the methyl stilbene mesogen. At the short end of this grouping, the extended -$(CH_2)_5$- length is only about 7.4 Å yet a stable intermeshed structure is still observed because the carbonate-pentane-carbonate length is about 11.8 Å. Here the carbonate linking group plays an important role in determining whether or not a stable intermeshed structure can be formed.

The carbonyl oxygen in the carbonate linkage is of partial negative charge while the remaining atoms in the carbonate linkage are of partial positive charge. This leads to a dipole moment transverse to the molecular chain axis at the position of the carbonate group. As shown in Figure 6, in HMS-5 and 7, consecutive carbonate dipoles on the chain point in nearly the same direction while in HMS-6 and 8 consecutive dipoles point in nearly opposite directions. This affects the way in which the corner and center chains are positioned relative to one another, and creates an odd-even effect in the packing of the cell. In HMS-5 and 7, the center and corner chains have dipole moments

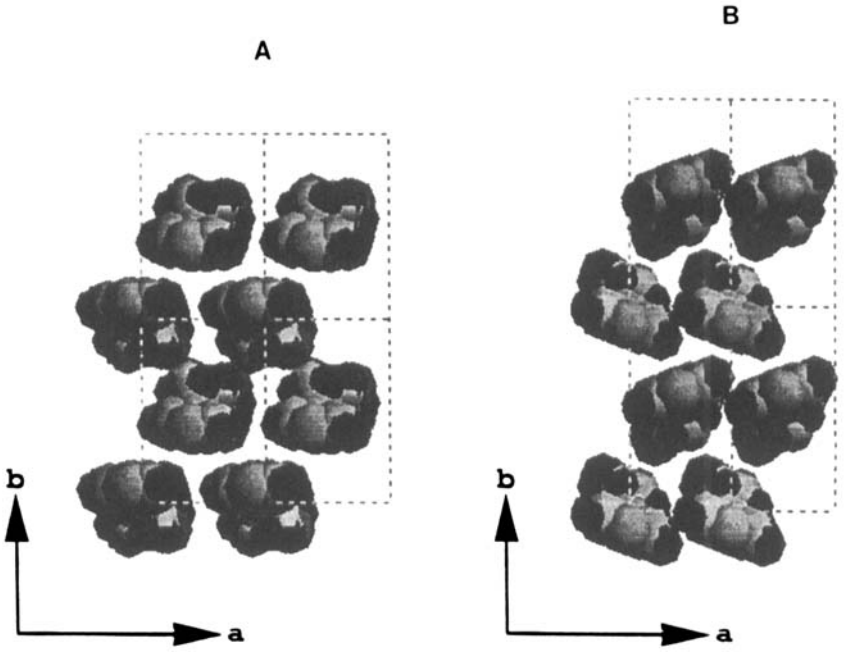

FIGURE 8 a) HMS-7, and b) HMS-8, projection view along the *c*-axis.

aligned, and pointing along [010]. In HMS-6 and 8, the dipole moments on adjacent carbonate units between chains can have a more favorable interaction when the center chain rotates relative to the corner chain. This rotation is demonstrated in Figure 8 where we show a view of the unit cells of HMS-7 and 8 for comparison, projected along the *c*-axis. The rotation of the adjacent chains of HMS-6 and 8, causes the length of the *b*-axis of the unit cell to increase, and the quantity $a \sin \beta$ to decrease, compared with HMS-5 and 7.

HMS-7 and 8 have a higher degree of overlap of the carbonate linkage between adjacent polymer chains than is found in HMS-5 and 6. This is caused by the very close match between the length of the mesogen and the length of the flexible spacer. We suggest this is the reason why HMS-7 and 8 have a less stable mesophase than HMS-5 and 6. As seen in the differential scanning calorimetry cooling studies,[6] the temperature stability range of the mesophase decreases from HMS-5 to 8. More over, as mentioned above, only a diffuse maximum is seen in the raw fiber pattern of HMS-5 and 6, which suggests that in the mesophase of these LCPs, the polymers chains arrange themselves randomly in two dimensions. The diffuse maximum represents the average distance between chains in the nematic mesophase. However, both HMS-7 and 8 show two spots on each side of the equator in the raw fiber pattern, which is evidence that in the mesophase of these two, there already exists a more regular arrangement of polymer chains in two dimensions. This would lead to faster crystallization from the mesophase, and therefore, mesophase of reduced stability.

4. CONCLUSIONS

HMS polycarbonates with 5 to 8 methylene flexible spacer units have a stable intermeshed crystal structure. Within this structure, the disposition of the carbonate group differs from *n*-even to *n*-odd and causes the odd-even effect of the crystal unit cell parameters, *b* and $a \sin \beta$. Furthermore, the higher degree of overlap of the carbonate linkage of HMS-7 and 8 than HMS-5 and 6 between adjacent polymer chains may be the reason why HMS-7 and 8 have less stable mesophase than HMS-5 and 6.

Acknowledgments

This research was supported by U.S. Army contract DAAL03-G-91-0134 and DAAH04-93-G-0347. PPG Industries Foundation is acknowledged for supporting acquisition of the Silicon Graphics Workstation used for molecular modeling studies. MVB thanks the NASA Graduate Research program for a graduate student fellowship during a portion of this research.

References

1. A. L. Bluhm, P. Cebe, H. L. Schreuder-Gibson, J. T. Stapler and W. Yeomans, *Mol. Cryst. Liq. Cryst.* **239**, 123 (1994).
2. E. C. Dobbs, L. Goldberg, W. Lawson and R. Robinson, *Proc. Roy. Soc.* **B127**, 140 (1939).
3. V. Percec, T. D. Shaffer and H. Nava, *J. Polym. Sci., Polym. Lett.* **22**, 637 (1984).
4. A. Ruviello and A. Sirigu, *Makromol. Chem.* **183**, 895 (1982).
5. A. Blumstein, *Polym. J.* **17(1)**, 277 (1985).

6. Y.-Y. Cheng, P. Cebe, H. Schreuder-Gibson, A. Bluhm and W. Yeomans, *Macromolecules* **27**, 5440 (1994).
7. R. Pardey, A. Zhang, P. A. Gabori, F. W. Harris, S. Z. D. Cheng, J. Adduci, J. V. Facinelli and R. W. Lenz, *Macromolecules* **25**, 5060 (1992).
8. F. Papadimitrakopoulos, S. L. Hsu and W. J. MacKnight, *Macromolecules* **25**, 4761 (1992).
9. F. Papadimitrakopoulos, E. Sawa and W. J. MacKnight, *Macromolecules* **25**, 4682 (1992).
10. V. Percec and Y. Tsuda, *Macromolecules* **23**, 3509 (1990).
11. V. Percec and R. Yourd, *Macromolecules* **22**, 524 (1989).
12. V. Percec and R. Yourd, *Macromolecules* **22**, 3229 (1989).
13. S. Z. D. Cheng, M. A. Yandrasits and V. Percec, *Polymer* **32**, 1284 (1991).
14. M. Yandrasits, S. Z. D. Cheng, A. Zhang, J. Cheng, B. Wunderlich and V. Percec, *Macromolecules* **25**, 2112 (1992).
15. K. Fujishiro and R. W. Lenz, *Macromolecules* **25**, 81 (1992).
16. V. Percec and A. Keller, *Macromolecules* **23**, 4347 (1990).
17. R. B. Blumstein and A. Blumstein, *Mol. Cryst. Liq. Cryst.* **165**, 361 (1988).
18. A. Blumstein and O. Thomas, *Macromolecules* **15**, 1264 (1982).
19. A. Blumstein, *Polym. J.* **17(1)**, 277 (1985).
20. A. M. Donald and A. H. Windle, *Liquid Crystalline Polymers* (Cambridge University Press, Cambridge, 1992), Chap. 3.
21. A. Abe, *Macromolecules* **17**, 2280 (1984).
22. D. Y. Yoon and S. Bruckner, *Macromolecules* **18**, 651 (1985).
23. P. Cebe, J. Carbeck and H. Schreuder-Gibson, *Polym. Preprints* **33(1)**, 331 (1992).
24. M. Sato, K. Nakatsuchi and Y. Ohkatsu, *Makromol. Chem., Rapid Commun.* **7**, 231 (1986).
25. G. Unger and A. Keller, *Mol. Cryst. Liq. Cryst.* **155**, 313 (1988).
26. A. Biswas, K. H. Gardner and P. W. Wojtkowski, in *Liquid-Crystalline Polymers* (Ed., R. A. Weiss and C. K. Ober, American Chemical Society, 1990), Chap. 19. pp. 256–268.